Journal of Computational Physics 401 (2020) 108975

Contents lists available at ScienceDirect

Journal of Computational Physics

www.elsevier.com/locate/jcp

Two classes of linearly implicit local energy-preserving approach for general multi-symplectic Hamiltonian PDEs

Jiaxiang Cai [a], Jie Shen [b,*]

[a] School of Mathematical Science, Huaiyin Normal University, Huaian, Jiangsu 223300, China
[b] Department of Mathematics, Purdue University, West Lafayette, IN, 47907, USA

ARTICLE INFO

Article history:
Received 15 May 2019
Received in revised form 19 September 2019
Accepted 20 September 2019
Available online 2 October 2019

Keywords:
Multi-symplectic
Hamiltonian PDE
Energy-preserving
Stability
IEQ

ABSTRACT

Two classes of efficient and robust schemes are proposed for the general multi-symplectic Hamiltonian systems using the invariant energy quadratization (IEQ) approach. The schemes are linear, second-order accurate, local energy-preserving, and preserve the global energy. They are not restricted to specific forms of the nonlinear part of the state function, and only require solving linear equations at each time step. We applied the new schemes to various multi-symplectic Hamiltonian PDEs to demonstrate their effectiveness, computational efficiency and accuracy.

1. Introduction

Many problems in sciences and engineering can be described by PDEs in the form of multi-symplectic Hamiltonian systems [4]:

$$M\partial_t z + \sum_{l=1}^{d} K_l \partial_{x_l} z = \nabla_z S(z), \quad z \in \mathbb{R}^{d_1}, \tag{1}$$

where M and K_l, $l = 1, 2, \ldots, d$, are constant $d_1 \times d_1$ skew-symmetric matrices, $z = z(t, \mathbf{x})$, $\mathbf{x} = (x_1, x_2, \ldots, x_d)$, is a state variable, and $S : \mathbb{R}^{d_1} \to \mathbb{R}$ is a scalar-valued smooth state function. Examples include KdV equation, Camassa-Holm equation, Sine-Gordon equation, Schrödinger equation, Klein-Gordon-Schrödinger equations, Zakharov-Kuznetsov equation, Maxwell's equations and so on [2,5–7,14,16,20,24,37].

It's well-known that the solution z of the system (1) admits a multi-symplectic conservation law (MSCL) [4]

$$\partial_t \omega + \sum_{l=1}^{d} \partial_{x_l} \kappa_l = 0, \tag{2}$$

where $\omega = dz \wedge \widehat{M} dz$ and $\kappa_l = dz \wedge \widehat{K}_l dz$. Here, the matrices $\widehat{M}$ and $\widehat{K}_l$ satisfy

* Corresponding author.
E-mail address: shen7@purdue.edu (J. Shen).

https://doi.org/10.1016/j.jcp.2019.108975
0021-9991/

$$M = \widehat{M} - \widehat{M}^T, \quad K_l = \widehat{K}_l - \widehat{K}_l^T. \tag{3}$$

Besides the MSCL, the solution z of (1) also satisfies the local energy conservation law (LECL)

$$\partial_t E + \sum_{l=1}^{d} \partial_{x_l} F_l = 0, \tag{4}$$

where $E = S(z) + \sum_{l=1}^{d} (\partial_{x_l} z)^T \widehat{K}_l z$ and $F_l = -(\partial_t z)^T \widehat{K}_l z$ are the energy density and fluxes, respectively, and the local momentum conservation law (LMCL) in each of the x_l-direction ($l = 1, 2, \ldots, d$):

$$\partial_t I_l + \partial_{x_l} G_l + \sum_{j=1, j\neq l}^{d} \partial_{x_j} \tilde{G}_{l,j} = 0,$$

where $I_l = -(\partial_{x_l} z)^T \widehat{M} z$, $G_l = S(z) + (\partial_t z)^T \widehat{M} z + \sum_{j=1, j\neq l}^{d} (\partial_{x_j} z)^T \widehat{K}_j z$ and $\tilde{G}_{l,j} = -(\partial_{x_l} z)^T \widehat{K}_j z$.

Many conservative evolutionary PDEs, under appropriate boundary conditions, can also be written as a general form

$$\partial_t u = \mathcal{D} \frac{\delta \mathcal{H}}{\delta u}, \tag{5}$$

where $\mathcal{D}$ is a constant skew symmetric linear differential operator, which preserves the global energy $\mathcal{H}$ and symplecticity.

However, the MSCL, LECL and LMCLs of the multi-symplectic Hamiltonian system (1) are local properties and independent of boundary conditions, since they are exact on any time-space point. If the system (1) is supplemented with appropriate boundary conditions such as periodic/homogenous boundary condition, then integrating MSCL, LECL and LMCLs over the space leads to symplecticity, global energy conservation and global momentum conservation, respectively. Thus, the system (1) is more general than the system (5). Actually, one can always write (5), with suitable boundary conditions, in the form (1). Schemes that conserve geometric structure (local structure or global invariants) are sometimes called geometric- or structure-preserving integrator, which are important for studying the long-term behavior of dynamical systems. Nowadays, preservation of some invariants or system structures has been a criterion to judge the success of the numerical scheme.

In the last decade, many systematic methodologies (also called multi-symplectic integrators) holding the discrete version of the MSCL have been proposed for the system (1) in one dimension, such as the box/Preissmann scheme [26], the Euler-box scheme [30], the Fourier pseudo-spectral collocation scheme [14], the wavelet collocation scheme [43] and the diamond scheme [29]. These multi-symplectic integrators have been successfully applied to the Schrödinger-type equations [14,21], KdV equation [2], RLW equation [7], the Camassa-Holm equation [16], Maxwell's equations [24,38] and so on. For more details, one can refer to the review paper [26] and references therein. While multi-symplectic-preserving methods do have some remarkable advantages such as suitability for long-term integrations, they do not typically preserve energy and momentum, which can be important for stability and convergence analysis.

Recently, designing numerical schemes preserving certain structure, especially the energy structure, for the continuous dynamical systems have attracted much attention [8,13,25,33]. The local structure produces richer information of the PDE system than the corresponding global one does, since the former does not need the appropriate boundary conditions while the latter does. In general, the conservative methods preserving global invariants are invalid for the problem without appropriate boundary conditions. Since LECL is an important local structure for the system (1), many works have been devoted to preserve it in the discrete version. In [39], Wang et al. made use of the concatenating idea to construct local energy-preserving (LEP) schemes for the one-dimensional (1D) Sine-Gordon equation. This technique was also employed to develop LEP schemes for the coupled nonlinear Schrödinger equations [11] and the Cahn-Hilliard equation [31]. The concatenating method can result in several different LEP schemes for a given conservative/dissipative PDEs, but it is not systematic either in derivations or in applicability to a class of PDEs. Furthermore, these LEP schemes are all fully implicit. In [12,18], we employed the averaged vector field (AVF) method [28,32] for constructing LEP integrators, respectively,

$$M\delta_t A_x^+ z_j^n + K_1 \delta_x^+ A_t z_j^n = \int_0^1 \nabla S(\xi A_x^+ z_j^{n+1} + (1-\xi) A_x^+ z_j^n)) \mathrm{d}\xi, \tag{6}$$

and

$$M\delta_t z_j^n + \widehat{K}_1 \delta_x^+ A_t z_j^n + \widehat{K}_1 \delta_x^- A_t z_j^n = \int_0^1 \nabla S(\xi z_j^{n+1} + (1-\xi) z_j^n)) \mathrm{d}\xi, \tag{7}$$

where the definitions of operators δ_t, $\delta_x^{\pm}$, A_t and A_x^+ can be found in Section 2, which is applicable to the entire class (1) in one dimension. The two LEP integrators have been successfully applied to many PDEs and the resulting schemes exhibited excellent performance in providing accurate solution and preserving the local/global energy. However, these schemes are always fully implicit, so they are very expensive, particularly when applied to the multi-dimensional systems (1).

From the performance perspective, a scheme for the multi-symplectic Hamiltonian system (1) is generally evaluated from the following aspects: whether it preserves the local energy conservation law; the order of its accuracy; its efficiency; whether it is easy to implement. Obviously, the existing structure-preserving schemes, including the MS schemes and LEP schemes, have shortcomings in the last two aspects due to their fully implicit feature. Besides, for these fully implicit conservative schemes, exact preservation of the invariant requires that the nonlinear system be solved to machine precision, this procedure can be very time-consuming. Thus it is highly desirable to have linearly implicit conservative schemes. In [17,27], for the conservative PDEs with polynomial nonlinearities, the authors developed a framework for constructing linearly implicit method conserving a time discretized version of energy by combining polarization of the energy and the discrete variational derivatives or AVF method. However, these methodologies are invalid for the conservative PDEs with non-polynomial nonlinearities or the multi-component polynomial nonlinearities such as the multi-symplectic Hamiltonian system (1). In [34,35], Shen et al. proposed linearly implicit schemes for the gradient flow by introducing the scalar auxiliary variable (SAV). The SAV approach is flexible and applicable to a large class of dissipative/conservative system, but it cannot preserve local structures for the multi-symplectic Hamiltonian system.

In this study, we develop linearly implicit LEP methods that are applicable to the entire class of multi-symplectic Hamiltonian PDEs (1). Inspired by the IEQ approach [40,41], we modify the state function in (1) into a quadratic form $S(z) = S_1(z) + r^2$ by introducing the auxiliary variable $r = \sqrt{S_2(z) + C_0}$ (see Section 2.1), and rewrite the original multi-symplectic Hamiltonian system (1) into a new equivalent system. By adopting some special discretizations in space and Crank-Nicolson discretization in time for the new system, we develop two classes of LEP integrators for the multi-symplectic system (1) which preserve the discrete version LECL exactly. These schemes possess the following remarkable advantages:

- For any PDE in the class of multi-symplectic Hamiltonian systems (1), one only needs to solve a linear system of equations at each time step, so that the schemes are remarkably efficient.
- The schemes are second-order in both time and space, and conserve the local and global energies.
- For some multi-component PDEs that belongs to multi-symplectic Hamiltonian system (1), such as Sine-Gordon (see Sec. 4), coupled nonlinear Schrödinger equations and so on, our schemes can be decoupled, so that one only needs to solve decoupled linear equations at each time for each of the components.

The rest of paper is organized as follows. In Section 2, we describe the two classes of linearly implicit LEP integrators for the 1D general multi-symplectic systems, and present their remarkable advantages. In Section 3, the methodologies for the 1D system are extended to the multi-symplectic Hamiltonian PDEs in d dimensions. In Section 4, we apply these new efficient integrators to solve various PDEs in the class of multi-symplectic Hamiltonian systems, and present ample numerical experiments to demonstrate their performance, followed by some concluding remarks in Section 5.

2. Linearly implicit LEP schemes for 1D systems

For clarity of presentation, we shall first present our methods for the multi-symplectic Hamiltonian PDE (1) in one dimension ($d = 1$), i.e.,

$$M\partial_t z + K\partial_x z = \nabla_z S(z), \quad z \in \mathbb{R}^{d_1}, \tag{8}$$

where $(x, t) \in [a, b] \times [0, T]$. The notations and methodologies in one-dimensional case will be generalized to the multi-symplectic Hamiltonian system (1) in multi dimensions in the next section.

We introduce some notations for dealing with the discrete systems. Let the notation u_j^n represent the approximation value of $u(a + jh, n\tau)$, where the index j corresponds to increments in space and n to increments in time, and $h = (b-a)/J$ and $\tau = T/N$. We also define the finite difference operators

$$\delta_t f_j^n = (f_j^{n+1} - f_j^n)/\tau, \quad \delta_x^{\pm} f_j^n = \pm(f_{j\pm1}^n - f_j^n)/h,$$

and the average operators

$$A_t f_j^n = (f_j^{n+1} + f_j^n)/2, \quad A_x^{\pm} f_j^n = (f_{j\pm1}^n + f_j^n)/2.$$

Obviously, these operators are commutative mutually, and also satisfy the following discrete Leibnitz rules

$$\begin{aligned}\delta_t(f_j^n \cdot g_j^n) =& \delta_t f_j^n \cdot A_t g_j^n + A_t f_j^n \cdot \delta_t g_j^n,\\ \delta_x^+(f_j^n \cdot g_j^n) =& \delta_x^+ f_j^n \cdot A_x^+ g_j^n + A_x^+ f_j^n \cdot \delta_x^+ g_j^n,\end{aligned}$$

and

$$\delta_x^+(f_{j-1}^n \cdot g_j^n) = f_j^n \cdot \delta_x^+ g_j^n + \delta_x^- f_j^n \cdot g_j^n.$$

2.1. The equivalent IEQ system

Usually, the scalar-valued state function $S(z)$ in (8) contains quadratic term and non-quadratic term, which can be written as

$$S(z) = S_1(z) + S_2(z),$$

where $S_1(z)$ and $S_2(z)$ represent quadratic and non-quadratic terms, respectively. Assuming that the function $S_2(z)$ is bounded from below, e.g., there exists a constant $C_0 > 0$ such that $S_2(z) \geq -C_0$, one can introduce an auxiliary variable $r(x,t;z) = \sqrt{S_2(z) + C_0}$, and then rewritten the multi-symplectic Hamiltonian system (8) as

$$M\partial_t z + K\partial_x z = \nabla_z S_1(z) + \frac{r}{\sqrt{S_2(z)+C_0}}\nabla_z S_2(z), \tag{9a}$$

$$r_t = \frac{1}{2\sqrt{S_2(z)+C_0}}\partial_t z^\top \nabla_z S_2(z). \tag{9b}$$

The above system is equivalent to the multi-symplectic Hamiltonian system (8) under the initial condition $r(x,0;z) = \sqrt{S_2(z)|_{t=0} + C_0}$. However, it allows more flexibility in time discretization.

Multiplying $\partial_t z^\top$ on both sides of Eq. (9a) together with the vanishment of the term $\partial_t z^\top M \partial_t z$, and r on both sides of (9b), we have

$$\partial_t z^\top K \partial_x z = \partial_t S_1(z) + \frac{r}{\sqrt{S_2(z)+C_0}}\partial_t z^\top \nabla_z S_2(z). \tag{10}$$

and

$$\partial_t r^2 = \frac{r}{\sqrt{S_2(z)+C_0}}\partial_t z^\top \nabla_z S_2(z) \tag{11}$$

Combining Eqs. (10) and (11) together with

$$\begin{aligned}\partial_t z^\top K \partial_x z =& \partial_t z^\top \widehat{K}\partial_x z - \partial_x z^\top \widehat{K}\partial_t z\\ =& \partial_x(\partial_t z^\top)\widehat{K}z - \partial_t(\partial_x z^\top)\widehat{K}z,\end{aligned}$$

we have the following:

Theorem 2.1. *The system (9) is local energy-preserving, and holds the local energy-energy conservation law*

$$\partial_t E + \partial_x F = 0, \quad E = S_1(z) + r^2 + \partial_x z^\top \widehat{K} z, \quad F = -\partial_t z^\top \widehat{K} z. \tag{12}$$

Furthermore, with appropriate boundary conditions such as periodic/homogeneous boundary conditions, the system possesses the global energy conservation

$$\mathrm{d}\mathcal{E}/\mathrm{d}t = 0, \quad \mathcal{E} = \int_a^b S_1(z) + r^2 + \partial_x z^\top \widehat{K} z \mathrm{d}x. \tag{13}$$

Remark 2.1. The purpose of introducing the auxiliary variable r is to make the state function quadratic. This allows us more flexibility in discretization. The local/global energy law (12) may be regarded as a modified form of the original one.

2.2. The first class of linearly implicit approach

We consider first the semi-discretization in time. A semi-implicit second-order scheme based on Crank-Nicolson discretization in time for the system (9) is

$$\begin{aligned}M\delta_t z^n + K\partial_x A_t z^n =& \overline{\nabla} S_1(z^{n+1}, z^n) + \frac{A_t r^n}{\sqrt{S_2(\widetilde{z}^{n+1/2})+C_0}}\nabla_z S_2(\widetilde{z}^{n+1/2}),\\ \delta_t r^n =& \frac{1}{2\sqrt{S_2(\widetilde{z}^{n+1/2})+C_0}}(\delta_t z^n)^\top \nabla_z S_2(\widetilde{z}^{n+1/2}),\end{aligned} \tag{14}$$

where $\widetilde{z}$ can be any explicit approximation of $z(t_{n+1/2})$ with an error of $\mathcal{O}(\tau^2)$, and $\overline{\nabla}$ is a discrete gradient of H, that is, a continuous function of $(\hat{z}, z)$ satisfying $\overline{\nabla}_z H(\hat{z}, z)^\top(\hat{z} - z) = H(\hat{z}) - H(z)$ and $\overline{\nabla}_z H(z,z) = \nabla_z H(z)$ [19,22,32]. Here we use the AVF discrete gradient method. In the above, we may let

$$\widetilde{z}^{n+1/2} = (3z^n - z^{n-1})/2 \tag{15}$$

be the second-order extrapolation.

Multiplying the first and the second equations of (14) with $(\delta_t z^n)^\top$ and $2A_t r^n$, respectively, we see that the above semi-implicit second-order system conserves the following semi-discrete energy conservation law

$$\delta_t E^n + \mathrm{d}F^{n+1/2}/\mathrm{d}x = 0, \quad E^n = S_1(z^n) + (r^n)^2 + (\partial_x z^n)^\top \widehat{K} z^n, \quad F^{n+1/2} = -(\delta_t z^n)^\top \widehat{K} A_t z^n. \tag{16}$$

Obviously, the above is a local property and independent of boundary conditions.

For the spatial discretization, one has many choices, such as finite difference method, finite element method, spectral method and so on. However, our interest of this study is to design local energy-preserving schemes for the general multi-symplectic Hamiltonian system. To this end, applying the midpoint rule in space to the system (14) yields the following linearly implicit full-discrete scheme (LI-LEP-1)

$$\begin{aligned} M\delta_t A_x^+ z_j^n + K\delta_x^+ A_t z_j^n =& \overline{\nabla} S_1(A_x^+ z_j^{n+1}, A_x^+ z_j^n) + \frac{A_t A_x^+ r_j^n}{\sqrt{S_2(A_x^+ \widetilde{z}_j^{n+1/2}) + C_0}} \nabla_z S_2(A_x^+ \widetilde{z}_j^{n+1/2}), \\ \delta_t A_x^+ r_j^n =& \frac{1}{2\sqrt{S_2(A_x^+ \widetilde{z}_j^{n+1/2}) + C_0}} (\delta_t A_x^+ z_j^n)^\top \nabla_z S_2(A_x^+ \widetilde{z}_j^{n+1/2}), \end{aligned} \tag{17}$$

where $\widetilde{z}_j^{n+1/2} = (3z_j^n - z_j^{n-1})/2$.

Theorem 2.2. *The full-discrete scheme (17) is local energy-preserving, which possesses the discrete local energy conservation law*

$$\delta_t E_{j+1/2}^n + \delta_x^+ F_j^{n+1/2} = 0, \tag{18}$$

where $E_{j+1/2}^n = S_1(A_x^+ z_j^n) + (A_x^+ r_j^n)^2 + (\delta_x^+ z_j^n)^\top \widehat{K} A_x^+ z_j^n$ *and* $F_j^{n+1/2} = -(\delta_t z_j^n)^\top \widehat{K} A_t z_j^n$.

Proof. Multiplying the first and second equations of (17) with $(\delta_t A_x^+ z_j^n)^\top$ and $2A_t A_x^+ r^n$, respectively, and then combining the two obtained equations, we have

$$(\delta_t A_x^+ z_j^n)^\top K \delta_x^+ A_t z_j^n = \delta_t \left(S_1(A_x^+ z_j^n) + (A_x^+ r_j^n)^2 \right). \tag{19}$$

Thanks to the discrete Leibnitz rules $\delta_x^+(f_j^n \cdot g_j^n) = \delta_x^+ f_j^n \cdot A_x^+ g_j^n + A_x^+ f_j^n \cdot \delta_x^+ g_j^n$, the left term

$$\begin{aligned} (\delta_t A_x^+ z_j^n)^\top K \delta_x^+ A_t z_j^n =& (\delta_t A_x^+ z_j^n)^\top \widehat{K} \delta_x^+ A_t z_j^n - (\delta_x^+ A_t z_j^n)^\top \widehat{K} \delta_t A_x^+ z_j^n \\ =& (\delta_t A_x^+ z_j^n)^\top \widehat{K} \delta_x^+ A_t z_j^n - \delta_t \left((\delta_x^+ z_j^n)^\top \widehat{K} A_x^+ z_j^n \right) + (\delta_t \delta_x^+ z_j^n)^\top \widehat{K} A_t A_x^+ z_j^n \\ =& \delta_x^+ \left((\delta_t z_j^n)^\top \widehat{K} A_t z_j^n \right) - \delta_t \left((\delta_x^+ z_j^n)^\top \widehat{K} A_x^+ z_j^n \right). \end{aligned} \tag{20}$$

This completes the proof. □

2.3. The second class of linearly implicit approach

The linearly implicit LI-LEP-1 integrator is applicable to the entire class (8). However, the approximation of the solution z in space on the midpoint may be complicated for some PDEs, and it is usually difficult to carry out a rigorous error analysis. On the other hand, it is relatively easy to implement a scheme on the grid points and to carry out corresponding error analysis [3,9]. Hence, we propose another class of linearly implicit local energy-preserving scheme on the grid points for the multi-symplectic Hamiltonian system.

Let $\widehat{K}$ be an arbitrary splitting matrix of K, satisfying the relationship (3). We discretize the system (14) as follows (LI-LEP-2),

$$\begin{aligned} M\delta_t z_j^n + \widehat{K}\delta_x^+ A_t z_j^n - \widehat{K}^\top \delta_x^- A_t z_j^n =& \overline{\nabla} S_1(z_j^{n+1}, z_j^n) + \frac{A_t r_j^n}{\sqrt{S_2(\widetilde{z}_j^{n+1/2}) + C_0}} \nabla_z S_2(\widetilde{z}_j^{n+1/2}), \\ \delta_t r_j^n =& \frac{1}{2\sqrt{S_2(\widetilde{z}_j^{n+1/2}) + C_0}} (\delta_t z_j^n)^\top \nabla_z S_2(\widetilde{z}_j^{n+1/2}), \end{aligned} \tag{21}$$

where $\widetilde{z}_j^{n+1/2} = (3z_j^n - z_j^{n-1})/2$.

Theorem 2.3. *The semi-implicit scheme (21) possesses a discrete local energy conservation law*

$$\delta_t^+ E_j^n + \delta_x^+ F_j^{n+\frac{1}{2}} = 0, \tag{22}$$

where $E_j^n = S_1(z_j^n) + (r_j^n)^2 + (\delta_x^- z_j^n)^T \widehat{K} z_j^n$ *and* $F_j^{n+\frac{1}{2}} = -(\delta_t^+ z_{j-1}^n)^\top \widehat{K}(A_t z_j^n)$.

Proof. Multiplying the two equations of (21) with $(\delta_t z_j^n)^\top$ and $2A_t r_j^n$, respectively, one has

$$(\delta_t z_j^n)^\top \widehat{K}\delta_x^+ A_t z_j^n - (\delta_t z_j^n)^\top \widehat{K}^\top \delta_x^- A_t z_j^n = \delta_t \left(S_1(z_j^n) + (r_j^n)^2 \right).$$

By making use of the Leibnitz rule $\delta_x^+(f_{j-1}^n \cdot g_j^n) = f_j^n \cdot \delta_x^+ g_j^n + \delta_x^- f_j^n \cdot g_j^n$, the left term becomes

$$\begin{aligned}
&(\delta_t z_j^n)^\top \widehat{K}\delta_x^+ A_t z_j^n - (\delta_x^- A_t z_j^n)^\top \widehat{K}\delta_t z_j^n \\
=&(\delta_t z_j^n)^\top \widehat{K}\delta_x^+ A_t z_j^n - \delta_t \left((\delta_x^- z_j^n)^\top \widehat{K} z_j^n \right) + (\delta_t \delta_x^- z_j^n)^\top \widehat{K} A_t z_j^n \\
=&\delta_x^+ \left((\delta_t z_{j-1}^n)^\top \widehat{K} A_t z_j^n \right) - \delta_t \left((\delta_x^- z_j^n)^\top \widehat{K} z_j^n \right).
\end{aligned}$$

The proof is completed. □

We established above that both schemes are local energy preserving, as for the global energy, we have the following:

Theorem 2.4. *If the original multi-symplectic Hamiltonian system is subject to appropriate boundary conditions such that* $\sum_j \delta_x^+ F_j^{n+1/2} = 0$ *(for example, periodic or homogeneous Dirichlet boundary conditions), both the schemes (17) and (21) are global energy-preserving, i.e.,*

$$\mathcal{E}^n = \mathcal{E}^{n-1} = \ldots = \mathcal{E}^0, \tag{23}$$

where $\mathcal{E}^n = h\sum_j S_1(A_x^+ z_j^n) + (A_x^+ r_j^n)^2 + (\delta_x^+ z_j^n)^\top \widehat{K} A_x^+ z_j^n$ *for the former scheme and* $\mathcal{E}^n = h\sum_j S_1(z_j^n) + (r_j^n)^2 + (\delta_x^- z_j^n)^T \widehat{K} z_j^n$ *for the latter one.*

Proof. Summing the local energy conservation law (18) or (22) over spatial indices together with the boundary condition gives the corresponding global energy, immediately. □

Some remarks are in order:

- The Leibniz rule satisfied by the spatial discrete operators are crucial for designing local energy-preserving schemes.
- For a given multi-symplectic Hamiltonian PDE, one may get different linearly implicit local energy-preserving schemes from LI-LEP-2 (21) by different choices of the splitting matrix $\widehat{K}$, but LI-LEP-1 (17) leads to a unique scheme.
- While z and r in the LI-LEP-1 and LI-LEP-2 schemes appear to be coupled. However, one can usually eliminate r from the coupled system, leading to a linear equation for z only. We take LI-LEP-2 (21) as an example:
  - It follows from the second equation of (21) that $r_j^{n+1} = r_j^n + \frac{1}{2}(z_j^{n+1} - z_j^n)^\top \widetilde{a}_j^{n+1/2}$ where $\widetilde{a}_j^{n+1/2} = \nabla_z S_2(\widetilde{z}_j^{n+1/2}) / \sqrt{S_2(\widetilde{z}_j^{n+1/2}) + C_0}$.
  - Substituting the above representation of r_j^{n+1} into the first equation of (21) reads a scheme

$$M\delta_t z_j^n + \widehat{K}\delta_x^+ A_t z_j^n - \widehat{K}^\top \delta_x^- A_t z_j^n = \overline{\nabla} S_1(z_j^{n+1}, z_j^n) + \widetilde{a}_j^{n+1/2}(r_j^n + \frac{1}{4}(z_j^{n+1} - z_j^n)^\top \widetilde{a}_j^{n+1/2}) \tag{24}$$

    for solving z_j^{n+1}. Actually, for many PDEs, the scheme (24) can be simplified further by eliminating the auxiliary variables in z_j which are introduced to write the PDEs in multi-symplectic form (see Sec. 4).
- The linearly implicit LEP schemes (17) and (21) with (15) needs the initial values z^0 and z^1 to run. z^0 is determined from the given initial values and z^1 can be obtained from the schemes (17) and (21) with $\widetilde{z}_j^{n+1/2} = z_j^0 + z_j^1$.
- The schemes can be applied for multi-symplectic Hamiltonian systems with various types of nonlinearities.
- In this study, only one auxiliary variable r is introduced. For some problems, it may be advantageous to split the non-quadratic term into $S_2(z) + S_3(z) + \cdots + S_m(z)$ and introduces multiple auxiliary variables $r_k = \sqrt{S_k(z) + C_k}$, $k = 2, 3, \cdots, m$.

3. Extension to multi-dimensional systems

The methodology presented in the last section for 1-D systems can be easily extended to multi-dimensional systems, we will present the linearly implicit local energy-preserving schemes for the multi-symplectic systems (1) and their numerical properties without detailed discussion and derivation.

Consider the multi-symplectic Hamiltonian systems (1) with $\mathrm{x} \in \Omega = \Pi_{l=1}^{d}[a_l, b_l]$. Let $z^n_{j_1,\cdots,j_d}$ be a numerical approximation to $z(x_{1_{j_1}}, \cdots, x_{d_{j_d}}, t_n)$ where $x_{l\,j_l} = a_l + j_l h_l$, $h_l = (b_l - a_l)/J_l$, $j_l = 0, 1, \cdots, J_l$ and $l = 1, 2, \cdots, d$. For simplicity, if one of the indices is held constant, we will drop it from the notation, that is, $z := z^n_{j_1,\cdots,j_d}$, $z_{j_1-1} := z^n_{j_1-1,\cdots,j_d}$ and so on. Denote the forward and backward Euler finite difference operators in x_l direction by $\delta^+_{x_l}$ and $\delta^-_{x_l}$ respectively, and the forward and backward average operators in x_l direction by $A^+_{x_l}$ and $A^-_{x_l}$, respectively.

Assume that the state function $S(z) = S_1(z) + S_2(z)$ where $S_1(z)$ and $S_2(z)$ are defined as before. By introducing the auxiliary variable $r = \sqrt{S_2(z) + C_0}$, we have the following two classes of linearly implicit local energy-preserving schemes:

$$\begin{aligned} &M\delta_t \Pi_{k=1}^{d} A^+_{x_l} z + \sum_{l=1}^{d} K\delta^+_{x_l} \Pi^d_{k=1,k\neq l} A^+_{x_k} A_t z \\ =&\overline{\nabla} S_1(\Pi^d_{k=1} A^+_{x_k} z^{n+1}, \Pi^d_{k=1} A^+_{x_k} z^n) + \frac{\Pi^d_{k=1} A^+_{x_k} A_t r}{\sqrt{S_2\left(\Pi^d_{k=1} A^+_{x_k} \widetilde{z}^{n+1/2}\right) + C_0}} \nabla_z S_2\left(\Pi^d_{k=1} A^+_{x_k} \widetilde{z}^{n+1/2}\right), \\ &\delta_t \Pi^d_{k=1} A^+_{x_l} r = \frac{1}{2\sqrt{S_2\left(\Pi^d_{k=1} A^+_{x_k} \widetilde{z}^{n+1/2}\right) + C_0}} \left(\delta_t \Pi^d_{k=1} A^+_{x_k} z\right)^\top \nabla_z S_2\left(\Pi^d_{k=1} A^+_{x_k} \widetilde{z}^{n+1/2}\right) \end{aligned} \tag{25}$$

and

$$\begin{aligned} M\delta_t z + \sum_{l=1}^{d}\left(\widehat{K}_l \delta^+_{x_l} A_t z - \widehat{K}_l^\top \delta^-_{x_l} A_t z\right) =& \overline{\nabla} S_1(z^{n+1}, z^n) + \frac{A_t r}{\sqrt{S_2(\widetilde{z}^{n+1/2}) + C_0}} \nabla_z S_2(\widetilde{z}^{n+1/2}), \\ \delta_t r =& \frac{1}{2\sqrt{S_2(\widetilde{z}^{n+1/2}) + C_0}} (\delta_t z)^\top \nabla_z S_2(\widetilde{z}^{n+1/2}), \end{aligned} \tag{26}$$

where $\widetilde{z}^{n+1/2} = (3z^n - z^{n-1})/2$.

As in the 1D case, we can prove that the above schemes satisfy the discrete local energy conservation law

$$\delta_t E^n + \sum_{l=1}^{d} \delta^+_{x_l} F_l^{n+1/2} = 0, \tag{27}$$

where, for the scheme (25), $F_l^{n+1/2} = -(\delta_t \Pi^d_{k=1,k\neq l} A^+_{x_k} z)^\top \widehat{K}_l A_t \Pi^d_{k=1,k\neq l} A^+_{x_k} z$ and $E^n = S_1(\Pi^d_{k=1} A^+_{x_k} z) + (\Pi^d_{k=1} A^+_{x_k} r)^2 + \sum_{l=1}^{d} (\delta^+_{x_l} \Pi^d_{k=1,k\neq l} A^+_{x_k} z)^\top \widehat{K}_l \Pi^d_{k=1} A^+_{x_k} z$, and for the scheme (26), $E^n = S_1(z) + r^2 + \sum_{l=1}^{d} (\delta^-_{x_l} z)^T \widehat{K}_l z$ and $F_l^{n+\frac{1}{2}} = -(\delta_t^+ z_{j_l-1})^\top \widehat{K}_l (A_t z)$.

If the original multi-dimensional system is supplemented with periodic/homogeneous Dirichlet boundary conditions, summing up all spatial indexes in (27) gives global energy conservation

$$\mathcal{E}^n = h_1 h_2 \cdots h_d \sum_{j_1, j_2, \cdots, j_d} E^n = \cdots = \mathcal{E}^0 = h_1 h_2 \cdots h_d \sum_{j_1, j_2, \cdots, j_d} E^0. \tag{28}$$

4. Some applications

Many PDEs motivated by physics belong to the class of multi-symplectic Hamiltonian systems, including in particular the KdV equation, NLS-type equations, and Sine-Gordon equation. In this section, we apply our schemes to solve these equations with different boundary conditions.

In the following, we always take $\widehat{K}_l$ as an upper triangular matrix of the matrix K_l. At n-th time level, the solution error is calculated by $e_\infty = \|\mathrm{u}^n - u(t_n)\|_\infty$, the value of local energy is scaled by $\max_{j_1,\cdots,j_d} |\delta_t E^n + \sum_{l=1}^{d} \delta^+_{x_l} F_l^{n+1/2}|$, and the error in global energy is monitored by $\mathcal{E}^n - \mathcal{E}^0$.

4.1. The KdV equation

$$u_t + \eta u u_x + \mu^2 u_{xxx} = 0$$

can be written as a 1D multi-symplectic Hamiltonian system (8) with $S(z) = v^2/2 - uw + \eta u^3/6$, $z = (\phi, u, v, w)^T$ and

$$M = \begin{pmatrix} 0 & 1/2 & 0 & 0 \\ -1/2 & 0 & 0 & 0 \\ 0 & 0 & 0 & 0 \\ 0 & 0 & 0 & 0 \end{pmatrix}, \quad K = \begin{pmatrix} 0 & 0 & 0 & 1 \\ 0 & 0 & -\mu & 0 \\ 0 & \mu & 0 & 0 \\ -1 & 0 & 0 & 0 \end{pmatrix}.$$

Let $r = \sqrt{u^3 + C_0}$. An application of the LI-LEP-1 integrator (17) to the above form yields

$$\begin{cases} \frac{1}{2}\delta_t A_x^+ u_j^n + A_t \delta_x^+ w_j^n = 0, \\ -\frac{1}{2}\delta_t A_x^+ \phi_j^n - \mu A_t \delta_x^+ v_j^n = -A_t A_x^+ w_j^n + \frac{\eta A_t A_x^+ r_j^n}{2\sqrt{(A_x^+ \widetilde{u}_j^{n+1/2})^3 + C_0}} (A_x^+ \widetilde{u}_j^{n+1/2})^2, \\ \mu A_t \delta_x^+ u_j^n = A_t A_x^+ v_j^n, \quad A_t \delta_x^+ \phi_j^n = A_t A_x^+ u_j^n, \\ \delta_t A_x^+ r_j^n = \frac{3(A_x^+ \widetilde{u}_j^{n+1/2})^2}{2\sqrt{(A_x^+ \widetilde{u}_j^{n+1/2})^3 + C_0}} \delta_t A_x^+ u_j^n. \end{cases} \tag{29}$$

Since $\mu u_x = v$ and $\phi_x = u$ have no time derivative, $\mu \delta_x^+ u_j^n = A_x^+ v_j^n$ and $\delta_x^+ \phi_j^n = A_x^+ u_j^n$ are more accurate approximations for them than those in (29). Eliminating the auxiliary variables w_j^n, v_j^n and ϕ_j^n yields a linearly implicit scheme

$$\begin{cases} \delta_t (A_x^+)^3 u_j^n + \mu^2 (\delta_x^+)^3 A_t u_j^n + \frac{\eta}{2} \delta_x^+ A_x^+ \left(\frac{A_t A_x^+ r_j^n}{\sqrt{(A_x^+ \widetilde{u}_j^{n+1/2})^3 + C_0}} (A_x^+ \widetilde{u}_j^{n+1/2})^2 \right) = 0, \\ A_x^+ r_j^{n+1} = A_x^+ r_j^n + \frac{3(A_x^+ \widetilde{u}_j^{n+1/2})^2}{2\sqrt{(A_x^+ \widetilde{u}_j^{n+1/2})^3 + C_0}} (A_x^+ u_j^{n+1} - A_x^+ u_j^n). \end{cases} \tag{30}$$

Applying the LI-LEP-2 integrator to the problem reads

$$\begin{cases} \frac{1}{2}\delta_t u_j^n + \delta_x^+ A_t w_j^n = 0, \\ -\frac{1}{2}\delta_t \phi_j^n - \mu A_t \delta_x^+ v_j^n = -A_t w_j^n + \frac{\eta A_t r_j^n}{2\sqrt{(\widetilde{u}_j^{n+1/2})^3 + C_0}} (\widetilde{u}_j^{n+1/2})^2, \\ \mu \delta_x^- u_j^n = v_j^n, \quad \delta_x^- \phi_j^n = u_j^n, \\ \delta_t r_j^n = \frac{3(\widetilde{u}_j^{n+1/2})^2}{2\sqrt{(\widetilde{u}_j^{n+1/2})^3 + C_0}} \delta_t u_j^n, \end{cases}$$

which can also be written in a compact form

$$\begin{cases} \delta_t A_x^- u_j^n + \mu^2 \delta_x^+ \delta_x^- \delta_x^- A_t u_j^n + \frac{\eta}{2} \delta_x^- \left(\frac{A_t r_j^n}{\sqrt{(\widetilde{u}_j^{n+1/2})^3 + C_0}} (\widetilde{u}_j^{n+1/2})^2 \right) = 0, \\ r_j^{n+1} = r_j^n + \frac{3(\widetilde{u}_j^{n+1/2})^2}{2\sqrt{(\widetilde{u}_j^{n+1/2})^3 + C_0}} (u_j^{n+1} - u_j^n). \end{cases} \tag{31}$$

Next, we carried out some numerical experiments to test the numerical performance of the schemes ($C_0 = 1$). The KdV equation has a traveling wave solution $u(x,t) = 3c\,\mathrm{sech}^2(\frac{\sqrt{c}}{2}(x - ct - x_0))$, $-\infty < x < +\infty$, $c > 0$, which means the soliton initially at x_0 travels with velocity c and amplitude $3c$.

First, we perform simulations with the initial value $u_0(x) = u(x, 0)$ with $x \in [-40, 40]$, $c = 1/3$, $x_0 = 0$, periodic boundary condition, and parameters $\mu = \eta = 1$, $\tau = 0.05$, $h = 0.05$ and $T = 200$. With the periodic boundary condition, the exact solution becomes

$$u(x,t) = \begin{cases} 3c\,\mathrm{sech}^2\left(\frac{\sqrt{c}}{2}(x - f(t))\right), & x \in [-40 + f(t), 40], \\ 3c\,\mathrm{sech}^2\left(\frac{\sqrt{c}}{2}(x - f(t) + 80)\right), & x \in [-40, -40 + f(t)], \end{cases}$$

where $f(t) = \mathrm{mod}(ct, 80)$. The numerical results are illustrated with Fig. 1. The left hand graph shows both schemes have excellent long-term performance on solution, but LI-LEP-1 gives more accurate solution than LI-LEP-2. The right graphs show the local energy and global energy are conserved exactly, which verifies the theoretical results. Fig. 2 displays the behaviors of the original energy and modified energies that our schemes hold. One can see that each of the modified energy is a good approximation to the original energy. In the following numerical examples, since the original energy and modified energy have the similar behaviors, we will not show them again.

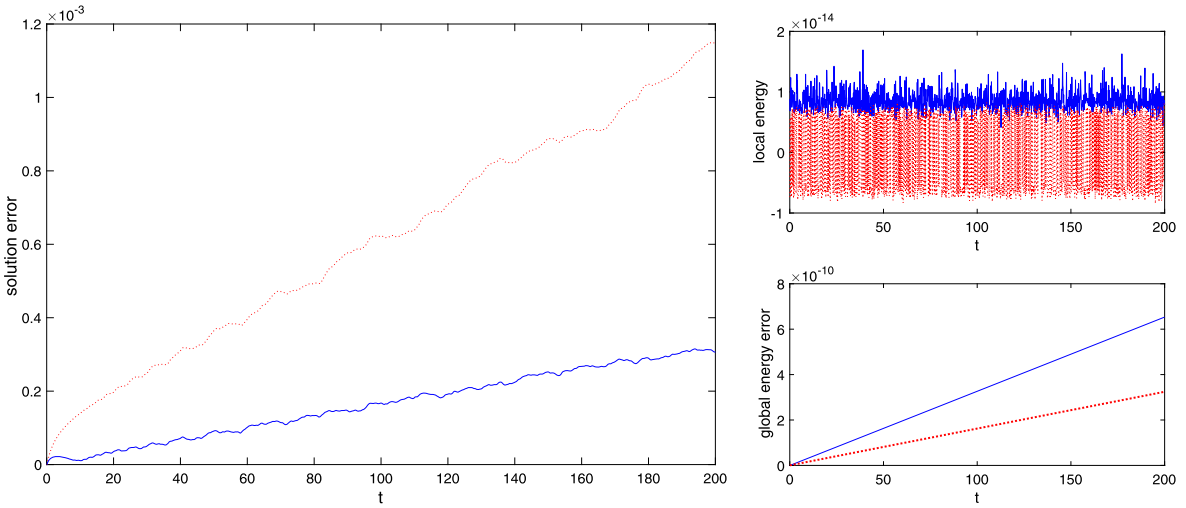

Fig. 1. Numerical results for the KdV equation given by (30) (solid line) and (31) (dotted line).

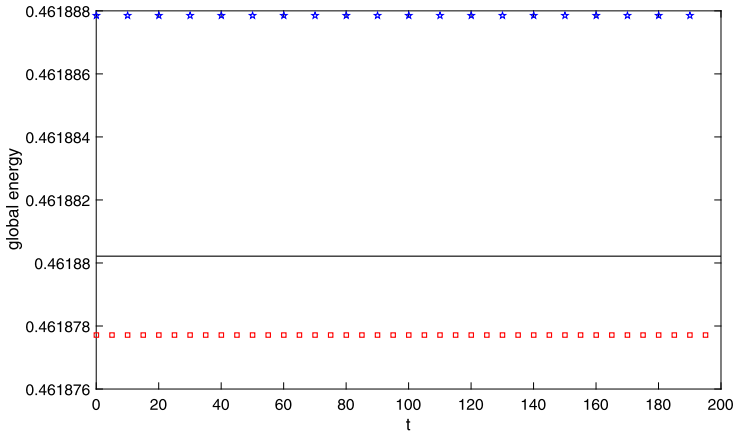

Fig. 2. The behaviors of the original energy (solid line) and the modified energies of schemes (squares: (30); stars: (31))

Table 1
Numerical results for the KdV equation at $T = 1$: $x \in [-40, 40]$, $\tau = h$.

Mesh	$\tau = 0.2$	$\tau/2$	$\tau/2^2$	$\tau/2^3$	$\tau/2^4$	$\tau/2^5$
LI-LEP-1	2.2510e-4	6.0011e-5	1.5420e-5	3.9058e-6	9.8264e-7	2.4598e-7
Order	–	1.9073	1.9604	1.9811	1.9909	1.9981
LI-LEP-2	4.5719e-4	1.2663e-4	3.3086e-5	8.4494e-6	2.1342e-6	5.3629e-7
Order	–	1.8522	1.9363	1.9693	1.9852	1.9926

Second, we test the convergence order of the solution. Table 1 displays the solution error and its convergence order in maximal error norm, in which the 'Order' is calculated by $\log(e_\infty(\tau_2)/e_\infty(\tau_1))/\log(\tau_2/\tau_1)$. The results confirm that both LI-LEP-1 and -2 have second order convergence in time and space.

Finally, we make numerical comparisons between our schemes and the existing second-order finite difference schemes, such as the LEP schemes [12,18], multi-symplectic Preissmann scheme (MPS) [42] and narrow box scheme (NBS) [1]. The results are listed in Table 2. It is clear that all schemes provide numerical solutions with similar accuracy (LI-LEP-1 has the most accurate solution), but the present schemes are much more efficient than the others.

4.2. Nonlinear Schrödinger equations

We consider first the 1D time-dependent NLS equation

$$\mathrm{i}\psi_t + \psi_{xx} + a|\psi|^2\psi = 0. \tag{32}$$

Table 2
Numerical results for the KdV equation: $x \in [-40, 40]$, $\tau = h = 0.05$, $T = 100$.

Results\Scheme	LI-LEP-1	LI-LEP-2	LEP-1[12]	LEP[18]	MPS[42]	NBS[1]
L_∞-error	1.67e-4	6.22e-4	3.83e-4	4.44e-4	4.50e-4	3.77e-4
$\lvert\mathcal{E}^n - \mathcal{E}^0\rvert$	9.62e-13	1.68e-12	1.06e-12	8.50e-12	2.25e-11	4.32e-5
CPU time	1.23 s	1.06 s	6.20 s	6.97 s	6.57 s	6.34 s

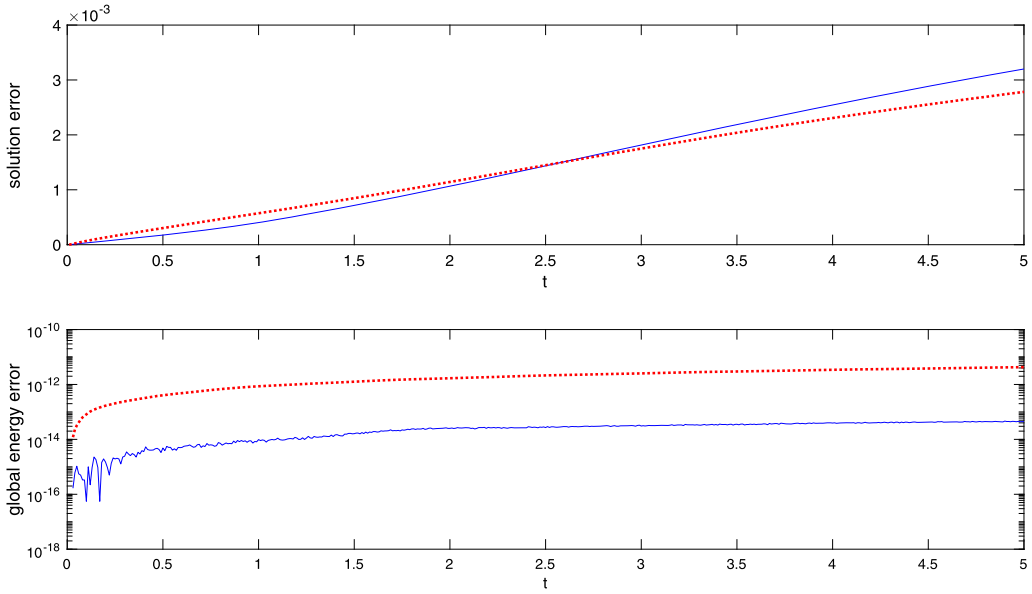

Fig. 3. Numerical results for 1D NLS equation (solid line: (33); dotted line: (34)). Top: the maximal error in solution; Bottom: global energy error.

By setting $\psi(x,t) = p(x,t) + iq(x,t)$, one obtains the multi-symplectic Hamiltonian form (8) with

$$S(z) = \frac{1}{2}(v^2 + w^2 + \frac{a}{2}(p^2+q^2)^2), \quad z = (p, q, v, w)^T$$

and

$$M = \begin{pmatrix} J & 0 \\ 0 & 0 \end{pmatrix}, K = \begin{pmatrix} 0 & -I \\ I & 0 \end{pmatrix}, J = \begin{pmatrix} 0 & 1 \\ -1 & 0 \end{pmatrix}, I = \begin{pmatrix} 1 & 0 \\ 0 & 1 \end{pmatrix}.$$

Let $r = \sqrt{(p^2+q^2)^2 + C_0}$. Then the LI-LEP-1 and LI-LEP-2 integrators lead to the following two linearly implicit local energy preserving schemes, respdectively,

$$\begin{cases} \mathrm{i}\delta_t A_x^+ A_x^- \psi_j^n + A_t \delta_x^+ \delta_x^- \psi_j^k + a A_x^- \left(A_t A_x^+ r_j^n A_x^+ \widetilde{\psi}_j^{n+1/2} \frac{|A_x^+ \widetilde{\psi}_j^{n+1/2}|^2}{\sqrt{|A_x^+ \widetilde{\psi}_j^{n+1/2}|^4 + C_0}} \right) = 0, \\ \delta_t A_x^+ r_j^n = \frac{2|A_x^+ \widetilde{\psi}_j^{n+1/2}|^2}{\sqrt{|A_x^+ \widetilde{\psi}_j^{n+1/2}|^4 + C_0}} \left(A_x^+ \Re(\widetilde{\psi}_j^{n+1/2}) \delta_t A_x^+ \Re(\psi_j^n) + A_x^+ \Im(\widetilde{\psi}_j^{n+1/2}) \delta_t A_x^+ \Im(\psi_j^n) \right), \end{cases} \tag{33}$$

and

$$\begin{cases} \mathrm{i}\delta_t \psi_j^n + A_t \delta_x^+ \delta_x^- \psi_j^k + a A_x^- \left(A_t r_j^n \widetilde{\psi}_j^{n+1/2} \frac{|\widetilde{\psi}_j^{n+1/2}|^2}{\sqrt{|\widetilde{\psi}_j^{n+1/2}|^4 + C_0}} \right) = 0, \\ \delta_t r_j^n = \frac{2|\widetilde{\psi}_j^{n+1/2}|^2}{\sqrt{|\widetilde{\psi}_j^{n+1/2}|^4 + C_0}} \left(\Re(\widetilde{\psi}_j^{n+1/2}) \delta_t \Re(\psi_j^n) + \Im(\widetilde{\psi}_j^{n+1/2}) \delta_t \Im(\psi_j^n) \right), \end{cases} \tag{34}$$

where $\Re$ and $\Im$ stand for the real and imaginary parts of complex function.

The NLS equation with $a = 2$ admits an analytical solution $\psi(x,t) = \mathrm{sech}(x - 2t)\exp(\mathrm{i}x)$. We run the above two schemes with initial condition $\psi(x,0) = \mathrm{sech}(x)\exp(\mathrm{i}x)$, $x \in [-20, 30]$ and periodic boundary condition. Fig. 3 displays the errors in solution and energy with $\tau = 0.01$ and $h = 0.02$. Obviously, LI-LEP-2 provides more accurate solution than LI-LEP-1 as $t > 2.5$, and both schemes preserve the energy exactly throughout the simulations. The results in Table 3 confirm the

Table 3
Numerical results for the Schrödinger equation at $T = 1$: $x \in [-20, 30]$, $\tau = h$.

Mesh	$\tau = 0.2$	$\tau/2$	$\tau/2^2$	$\tau/2^3$	$\tau/2^4$	$\tau/2^5$
LI-LEP-1	3.2955e-2	9.6676e-3	2.6671e-3	7.0030e-4	1.7950e-4	4.5444e-5
Order	–	1.7693	1.8579	1.9292	1.9640	1.9818
LI-LEP-2	1.1362e-1	3.1602e-2	8.3827e-3	2.1654e-3	5.4635e-4	1.3672e-4
Order	–	1.8461	1.9145	1.9528	1.9867	1.9986

Table 4
Numerical results for the Schrödinger equation: $x \in [-20, 30]$, $\tau = 0.01$, $h = 0.02$ and $T = 5$.

Results\Scheme	LI-LEP-1	LI-LEP-2	LEP-1 [12]	LEP-2 [12]	LEP [18]	LMP [18]
L_∞-error	3.20e-3	2.78e-3	1.40e-3	6.16e-3	4.74e-3	4.41e-3
$\lvert\mathcal{E}^n - \mathcal{E}^0\rvert$	8.55e-14	4.26e-12	2.91e-13	7.79e-13	6.27e-13	1.89e-7
CPU time	0.45 s	0.39 s	1.16 s	1.15 s	1.80 s	1.49 s

solutions of LI-LEP-1 and -2 converge to the exact solution with second order in time and space. Table 4 shows the numerical results of various schemes. All schemes have comparable solution accuracy, but our schemes consume the least CPU times.

Next we consider the 2D NLS equation

$$\mathrm{i}\psi_t + \alpha\Delta\psi + V'(|\psi|^2, \mathbf{x})\psi = 0, \tag{35}$$

where the symbol $'$ represents the derivative of V with respect to the first variable and the Laplace operator $\Delta = \partial^2_{x_1} + \partial^2_{x_2}$. With $\alpha = 1/2$ and $V(|\psi|^2, \mathbf{x}) = V_1(\mathbf{x})|\psi|^2 + \beta|\psi|^4/2$, Eq. (35) becomes Gross-Pitaevskii (G-P) equation which is an important mean field model for the dynamics of a dilute gas Bose-Einstein condensate. G-P equation is attractive for $\beta > 0$ and repulsive for $\beta < 0$.

Introducing $\psi = p + \mathrm{i}q$ again, the equation can be written into the multi-symplectic Hamiltonian form (1) with $S(z) = \frac{1}{2}V(p^2 + q^2, \mathbf{x}) + \frac{\alpha}{2}((v^{x_1})^2 + (w^{x_1})^2 + (v^{x_2})^2 + (w^{x_2})^2)$, $z = (p, q, v^{x_1}, w^{x_1}, v^{x_2}, w^{x_2})$, and the skew-symmetric matrices ($\in \mathbb{R}^{6\times 6}$)

$$M = \begin{pmatrix} J & 0 & 0 \\ 0 & 0 & 0 \\ 0 & 0 & 0 \end{pmatrix},\ K_1 = \begin{pmatrix} 0 & -\alpha I & 0 \\ \alpha I & 0 & 0 \\ 0 & 0 & 0 \end{pmatrix},\ K_2 = \begin{pmatrix} 0 & 0 & -\alpha I \\ 0 & 0 & 0 \\ \alpha I & 0 & 0 \end{pmatrix},$$

with matrices J, $I \in \mathbb{R}^{2\times 2}$ being the same as those in Example 2.

Introduce auxiliary variable $r = \sqrt{V(|\psi|^2, \mathbf{x}) + C_0}$, the LI-LEP-2 integrator to the equation yields the following linearly implicit scheme

$$\begin{cases} \mathrm{i}\delta_t\psi^n_{j_1,j_2} + \alpha\underline{\Delta}A_t\psi^k_{j_1,j_2} + aA^-_x\left(A_t r^n_{j_1,j_2}\widetilde{\psi}^{n+1/2}_{j_1,j_2}\dfrac{V'\left(|\widetilde{\psi}^{n+1/2}_{j_1,j_2}|^2, \mathrm{x}_{j_1,j_2}\right)}{\sqrt{V\left(|\widetilde{\psi}^{n+1/2}_{j_1,j_2}|^2, \mathrm{x}_{j_1,j_2}\right)+C_0}}\right) = 0, \\ \delta_t r^n_{j_1,j_2} = \dfrac{V'\left(|\widetilde{\psi}^{n+1/2}_{j_1,j_2}|^2, \mathrm{x}_{j_1,j_2}\right)}{\sqrt{V\left(|\widetilde{\psi}^{n+1/2}_{j_1,j_2}|^2, \mathrm{x}_{j_1,j_2}\right)+C_0}}\left(\Re(\widetilde{\psi}^{n+1/2}_{j_1,j_2})\delta_t\Re(\psi^n_{j_1,j_2}) + \Im(\widetilde{\psi}^{n+1/2}_{j_1,j_2})\delta_t\Im(\psi^n_{j_1,j_2})\right), \end{cases} \tag{36}$$

where $\underline{\Delta} = \delta^+_{x_1}\delta^-_{x_1} + \delta^+_{x_2}\delta^-_{x_2}$.

First, we simulate the attractive case with $\beta = 1$, $V_1(\mathbf{x}) = -(x_1^2 + x_2^2)/2 - 2\exp(-(x_1^2 + x_2^2))$, the initial condition $\psi(\mathbf{x}, 0) = \sqrt{2}\exp(-(x_1^2 + x_2^2)/2)$, $\mathrm{x} \in [-6, 6]^2$ and periodic boundary conditions. For this initial problem, the G-P equation has an exact solution $\psi(\mathbf{x}, t) = \sqrt{2}\exp(-(x_1^2 + x_2^2)/2 - \mathrm{i}t)$. The simulation is carried out with $h_1 = h_2 =$5e-2 and $\tau =$5e-4 till $T = 5$. Fig. 4 shows the variation of the solution error and global energy error of LI-LEP-2 as time evolves. It is clear that LI-LEP-2 gives satisfactory solution and captures the discrete global energy exactly. The results listed in Table 5 verify the solution of our scheme converges to the exact solution with second order in time and space.

Then, we consider the repulsive case with $\beta = -2$, $V_1 = -(x_1^2 + x_2^2)/2$ and the initial condition $\psi(\mathbf{x}, 0) = \exp(-(x_1^2 + x_2^2)/2)/\sqrt{\pi}$. The simulation is done on the domain $\Omega = [-8, 8]^2$ with $\tau =$5e-4 and $h_1 = h_2 =$5e-2 till $T = 5$. The profile of solution $|\psi|$ at $T = 5$ is illustrated with Fig. 5 (left). The right graph in Fig. 5 shows the global energy is preserved exactly again.

4.3. Sine Gordon equations

The results in the previous examples confirm the excellent performance of our schemes for the equations with periodic boundary conditions. Now we consider the Sine Gordon equations.

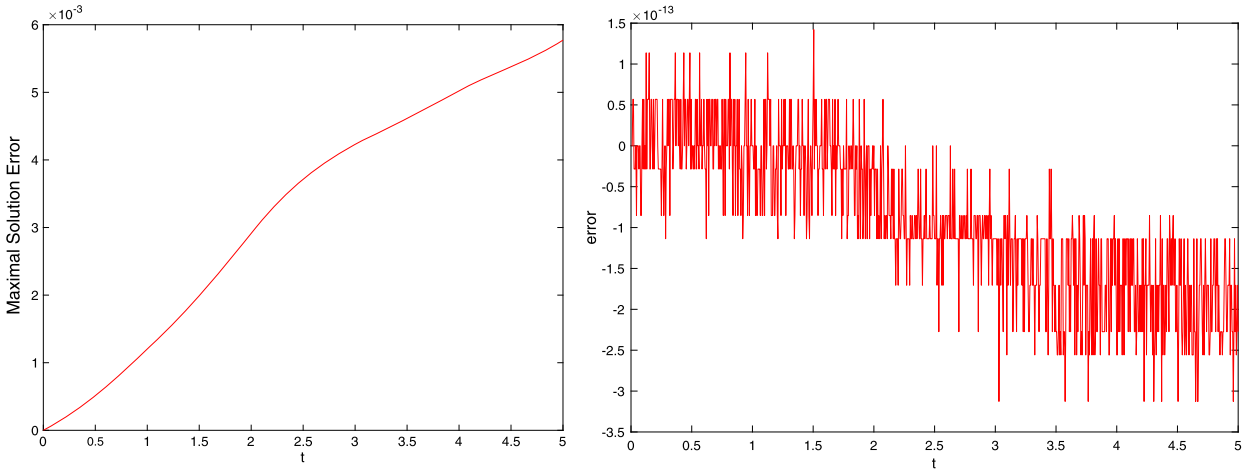

Fig. 4. Numerical results for the G-P equation (attractive case, $\beta = 1$). Left: the maximal error in solution; Right: the global energy error.

Table 5
Numerical results for the 2D G-P equation at $T = 1$: τ_0 =2e-3, $h_1 = h_2 = h_0$ =2e-1.

(τ, h)	(τ_0, h_0)	$(\tau_0, h_0)/2$	$(\tau_0, h_0)/2^2$	$(\tau_0, h_0)/2^3$	$(\tau_0, h_0)/2^4$
LI-LEP-2	1.9699e-2	4.8342e-3	1.2031e-3	3.0043e-4	7.5102e-5
Order	–	2.03	2.01	2.00	1.9640

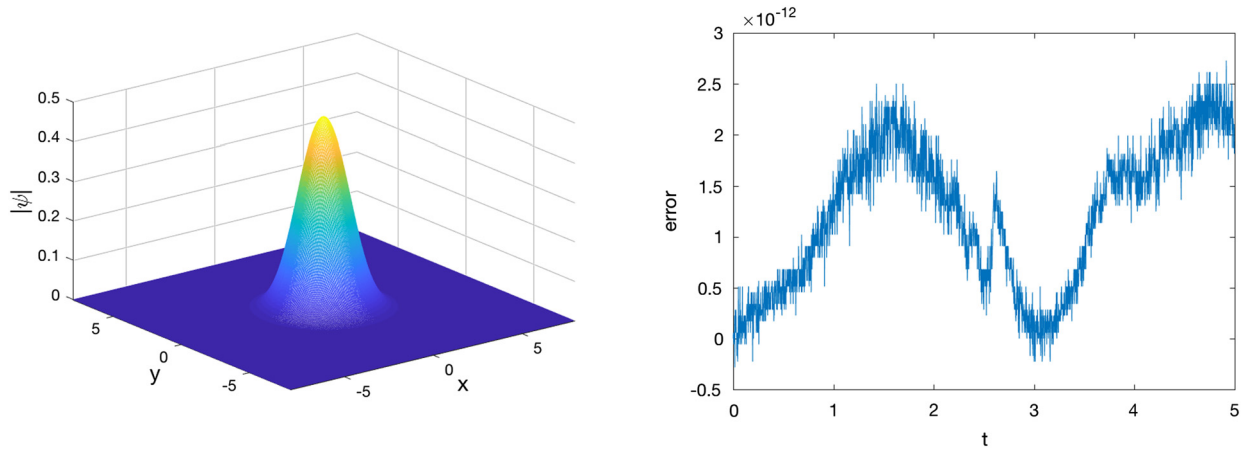

Fig. 5. Numerical results for the G-P equation (repulsive case, $\beta = -2$). Left: the profile of $|\psi|$ at $T = 5$. Right: the global energy error.

We first consider the 1D Sine-Gordon equation

$$u_{tt} - u_{xx} = -\sin u$$

with Dirichlet boundary condition. The above Sine-Gordon belongs to multi-symplectic Hamiltonian system with the state variable $z = (u, v, w)^\top$, the state function $S(z) = v^2/2 - w^2/2 - \cos u$ and skew-symmetric matrices

$$M = \begin{pmatrix} 0 & -1 & 0 \\ 1 & 0 & 0 \\ 0 & 0 & 0 \end{pmatrix}, \quad K = \begin{pmatrix} 0 & 0 & -1 \\ 0 & 0 & 0 \\ 1 & 0 & 0 \end{pmatrix}.$$

Let $r = \sqrt{C_0 - \cos u}$. The LI-LEP-1 scheme for the above problem reads to

$$\begin{cases} -\delta_t A_x^+ A_x^- v_j^n - A_t \delta_x^+ \delta_x^- w_j^n = \widetilde{a}_j^{n+1/2} A_t A_x^+ r, \\ \delta_t u_j^n = A_t v_j^n, \\ \delta_t A_x^+ r_j^n = \frac{1}{2} \widetilde{a}_j^{n+1/2} \delta_t A_x^+ u_j^n, \end{cases} \tag{37}$$

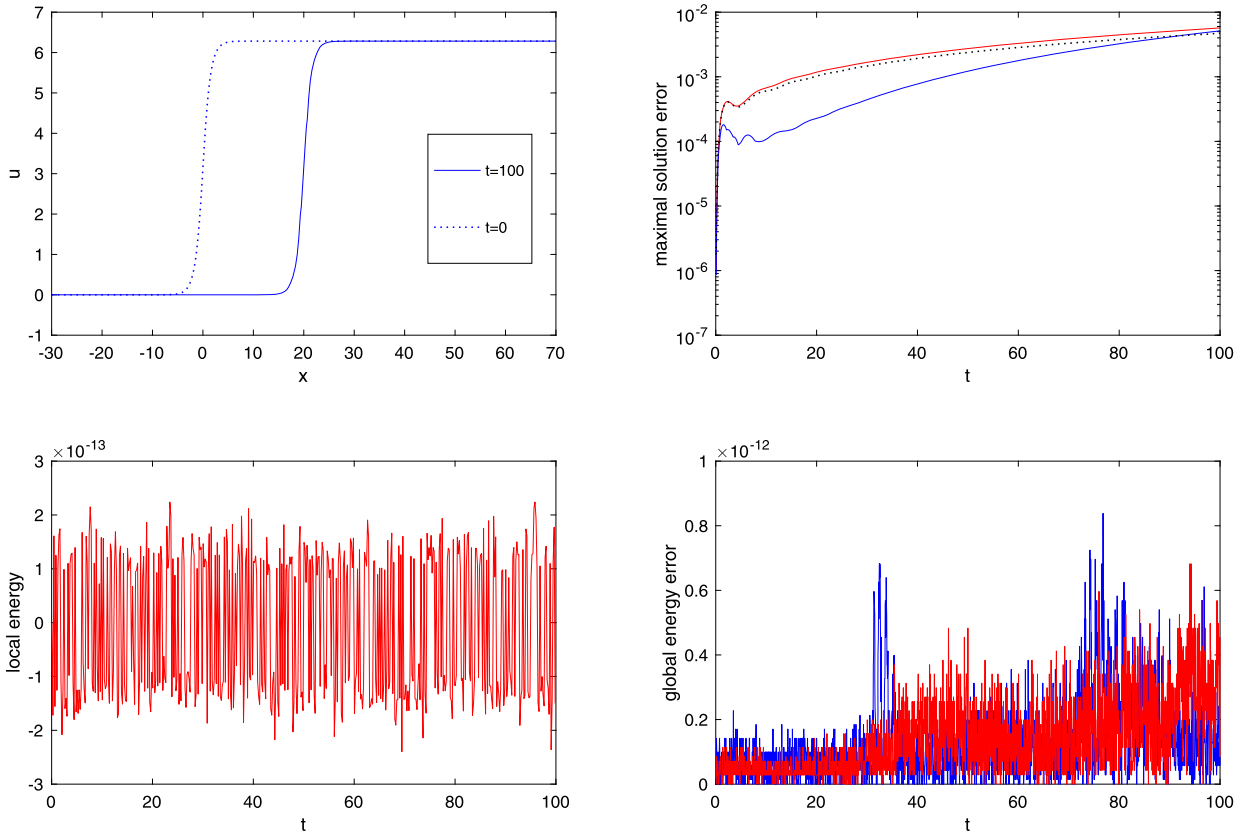

Fig. 6. The numerical results for 1D Sine-Gordon equation. Top-left: the solution at $t = 0$ and $t = 100$; Top-right: the solution error (bule line: LI-LEP-1; red line: LI-LEP-2; black dotted line: LEP [12]); Bottom-left: local energy of LI-LEP-2; Bottom-right: global energy error (bule line: LI-LEP-1; red line: LI-LEP-2).

This is a coupled scheme which can be cast into the following decoupled one

$$\begin{cases} -2\delta_t A_x^+ A_x^- u_j^n + \tau A_t \delta_x^+ \delta_x^- u_j^n = -2A_x^+ A_x^- v_j^n + \tau A_x^- \left(\widetilde{a}_j^{n+1/2} (A_x^+ r_j^n + \frac{\tau \widetilde{a}_j^{n+1/2}}{4} \delta_t A_x^+ u_j^n) \right), \\ v_j^{n+1} = \frac{2}{\tau}(u_j^{n+1} - u_j^n) - v_j^n, \\ A_x^+ r_j^{n+1} = A_x^+ r_j^n + \frac{\widetilde{a}_j^{n+1/2}}{2}(A_x^+ u_j^{n+1} - A_x^+ u_j^n), \end{cases} \tag{38}$$

where $\widetilde{a}_j^{n+1/2} = \sin(A_x^+ \widetilde{u}_j^{n+1/2}) / \sqrt{C_0 - \cos(A_x^+ \widetilde{u}_j^{n+1/2})}$.

On the other hand, application of the LI-LEP-2 scheme to the equation can be simplified to a decoupled one

$$\begin{cases} -2\delta_t u_j^n + \tau A_t \delta_x^+ \delta_x^- u_j^n = -2v_j^n + \tau \widetilde{a}_j^{n+1/2} \left(r_j^n + \frac{\widetilde{a}_j^{n+1/2}}{4}(u_j^{n+1} - u_j^n) \right), \\ v_j^{n+1} = \frac{2}{\tau}(u_j^{n+1} - u_j^n) - v_j^n, \\ r_j^{n+1} = r_j^n + \frac{\widetilde{a}_j^{n+1/2}}{2}(u_j^{n+1} - u_j^n), \end{cases} \tag{39}$$

where $\widetilde{a}_j^{n+1/2} = \sin(\widetilde{u}_j^{n+1/2}) / \sqrt{C_0 - \cos(\widetilde{u}_j^{n+1/2})}$.

The Sine-Gordon equation admits an analytical solution $u(x,t) = 4\arctan(\exp(\frac{x-ct}{\sqrt{1-c^2}}))$. We test our schemes with the initial conditions $u_0(x) = u(x,0)$ and $v_0(x) = u_t(x,0)$ where $x \in [-30, 70]$, $c = 0.2$, boundary conditions $u(-30,t) = u(-30,0)$ and $u(70,t) = u(70,0)$, and computational parameters $\tau = h = 0.05$ and $T = 100$. It should be noted that, for this problem, our schemes only need to solve linear equations with a tridiagonal coefficient matrix at each time step. Fig. 6 shows the obtained results on the waveform of solution, the maximal errors in solution, local energy and the errors in global energy. One can see that our linearly implicit LI-LEP-1 and LI-LEP-2 schemes have essentially the same solution accuracies as the fully implicit LEP scheme [12] at the final time $T = 100$, but consume much less CPU time. The results of the local energy

and global energy errors shown in the last two graphs confirm the theoretical results. All the results displayed in Fig. 6 indicate that our schemes can simulate the problem with general boundary condition well.

Next, we consider the Sine-Gordon equation in two dimensions

$$\begin{cases} u_{tt} - u_{xx} - u_{yy} = -\sin u, \ (x, y) \in \Omega = (a_1, b_1) \times (a_2, b_2), \\ u(x, y, 0) = f(x, y), \ \ u_t(x, y, 0) = v(x, y), \\ \nabla u \cdot \mathrm{n} = 0, \ (x, y) \in \partial\Omega, \end{cases}$$

where n is the outward unit normal of $\partial\Omega$.[1] The equation can be cast into the multi-symplectic Hamiltonian system (1) with the state variable $z = (u, v, w, \phi)^\top$, the state function $S(z) = (v^2 - w^2 - \phi^2)/2 - \cos u$ and skew-symmetric matrices

$$M = \begin{pmatrix} 0 & -1 & 0 & 0 \\ 1 & 0 & 0 & 0 \\ 0 & 0 & 0 & 0 \\ 0 & 0 & 0 & 0 \end{pmatrix}, \ K_1 = \begin{pmatrix} 0 & 0 & -1 & 0 \\ 0 & 0 & 0 & 0 \\ 1 & 0 & 0 & 0 \\ 0 & 0 & 0 & 0 \end{pmatrix}, \ K_2 = \begin{pmatrix} 0 & 0 & 0 & -1 \\ 0 & 0 & 0 & 0 \\ 0 & 0 & 0 & 0 \\ 1 & 0 & 0 & 0 \end{pmatrix}.$$

Let $r = \sqrt{C_0 - \cos u}$. Applying the LI-LEP-1 and LI-LEP-2 to this problem, respectively, gives the following two decoupled schemes

$$\begin{cases} -2\delta_t A^+_{xy} A^-_{xy} u^n_{j_1,j_2} + \tau \underline{\Delta} A_t u^n_{j_1,j_2} = -2A^+_{xy} A^-_{xy} v^n_{j_1,j_2} + \tau A^-_{xy} \left(\widetilde{a}^{n+1/2}_{j_1,j_2} (A^+_{xy} r^n_{j_1,j_2} + \frac{\tau \widetilde{a}^{n+1/2}_{j_1,j_2}}{4} \delta_t A^+_{xy} u^n_{j_1,j_2}) \right), \\ v^{n+1}_{j_1,j_2} = \frac{2}{\tau}(u^{n+1}_{j_1,j_2} - u^n_{j_1,j_2}) - v^n_{j_1,j_2}, \\ A^+_{xy} r^{n+1}_{j_1,j_2} = A^+_{xy} r^n_{j_1,j_2} + \frac{\widetilde{a}^{n+1/2}_{j_1,j_2}}{2} (A^+_{xy} u^{n+1}_{j_1,j_2} - A^+_{xy} u^n_{j_1,j_2}), \end{cases} \tag{40}$$

where $A^\pm_{xy} = A^\pm_x A^\pm_y$, $\underline{\Delta} = \delta^+_x \delta^-_x A^+_y A^-_y + A^+_x A^-_x \delta^+_y \delta^-_y$ and $\widetilde{a}^{n+1/2}_{j_1,j_2} = \sin(A^+_{xy} \widetilde{u}^{n+1/2}_{j_1,j_2}) / \sqrt{C_0 - \cos(A^+_{xy} \widetilde{u}^{n+1/2}_{j_1,j_2})}$, and

$$\begin{cases} -2\delta_t u^n_{j_1,j_2} + \tau \underline{\Delta} A_t u^n_{j_1,j_2} = -2v^n_{j_1,j_2} + \tau \widetilde{a}^{n+1/2}_{j_1,j_2} \left(r^n_{j_1,j_2} + \frac{\widetilde{a}^{n+1/2}_{j_1,j_2}}{4} (u^{n+1}_{j_1,j_2} - u^n_{j_1,j_2}) \right), \\ v^{n+1}_{j_1,j_2} = \frac{2}{\tau}(u^{n+1}_{j_1,j_2} - u^n_{j_1,j_2}) - v^n_{j_1,j_2}, \\ r^{n+1}_{j_1,j_2} = r^n_{j_1,j_2} + \frac{\widetilde{a}^{n+1/2}_{j_1,j_2}}{2} (u^{n+1}_{j_1,j_2} - u^n_{j_1,j_2}), \end{cases} \tag{41}$$

where $\underline{\Delta} = \delta^+_x \delta^-_x + \delta^+_y \delta^-_y$ and $\widetilde{a}^{n+1/2}_{j_1,j_2} = \sin(\widetilde{u}^{n+1/2}_{j_1,j_2}) / \sqrt{C_0 - \cos(\widetilde{u}^{n+1/2}_{j_1,j_2})}$.

There have been some simulations on the evolution of the circular ring solitons for the 2D Sine-Gordon equations in the literature [10,15,23,36]. We start with the initial conditions

$$u(x, y, 0) = 4 \arctan\left(\exp\left(3 - \sqrt{x^2 + y^2} \right) \right) \ \text{ and } \ v(x, y, 0) = 0, \ \ (x, y) \in [-14, 14]^2.$$

Here, we choose computational parameters $h_x = h_y = 28/399$ and $\tau = 0.1$. Fig. 7 displays the surfaces of the circular ring soliton in term of $\sin(u/2)$ at different times. One can see that the ring solitons shrink at the initial stage, but oscillations and radiations begin to form and continue slowly as time evolves. These results are consistent with those in the literature. The global energy errors of our schemes shown in the bottom-left graph are very close to zero.

Then, we simulate the interaction of two circular solitons by choosing initial data

$$\begin{aligned} u(x, y, 0) =& 4 \arctan\left(\exp(\gamma \chi_1) \right) + 4 \arctan\left(\exp(\gamma \chi_2) \right) \\ v(x, y, 0) =& 4.13 \ \mathrm{sech}(\gamma \chi_1) + 4.13 \ \mathrm{sech}(\gamma \chi_2), \end{aligned}$$

where $\gamma = 1/0.436$, $\chi_1 = 4 - \sqrt{(x+3)^2 + (y+7)^2}$, $\chi_2 = 4 - \sqrt{(x+17)^2 + (y+7)^2}$, $\Omega = [-30, 10] \times [-21, 7]$ and computational parameters $h_x = h_y = 40/199$ and $\tau = 0.1$ till $T = 8$. Fig. 8 shows that the two expanding circular ring solitons move in opposite directions, and then they interact, and finally they emerge into a large ring soliton. The obtained results again agree with the existing ones in the literature. The global energy errors shown in Fig. 9 show that our schemes do preserve the energy very well.

[1] In the schemes (40) and (41), the values on the ghost point outside the boundary are given by $u_{-1,j_2} = u_{1,j_2}$, $u_{J_1+1,j_2} = u_{J_1-1,j_2}$, $u_{j_1,-1} = u_{j_1,1}$ and $u_{j_1,J_2+1} = u_{j_1,J_2-1}$. The schemes cannot conserve the global energy exactly with this choice, but numerical results show that the schemes can preserve it very well.

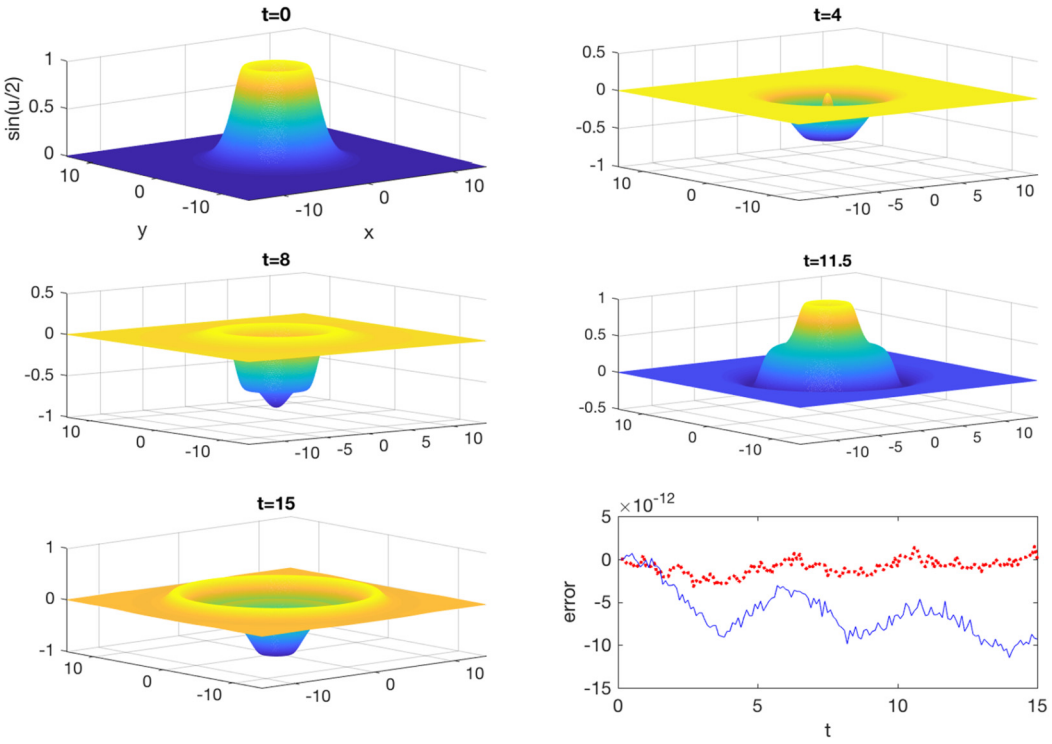

Fig. 7. The surface of the circular ring soliton ($\sin(u/2)$) and the error in energy (blue: LI-LEP-1, red: LI-LEP-2).

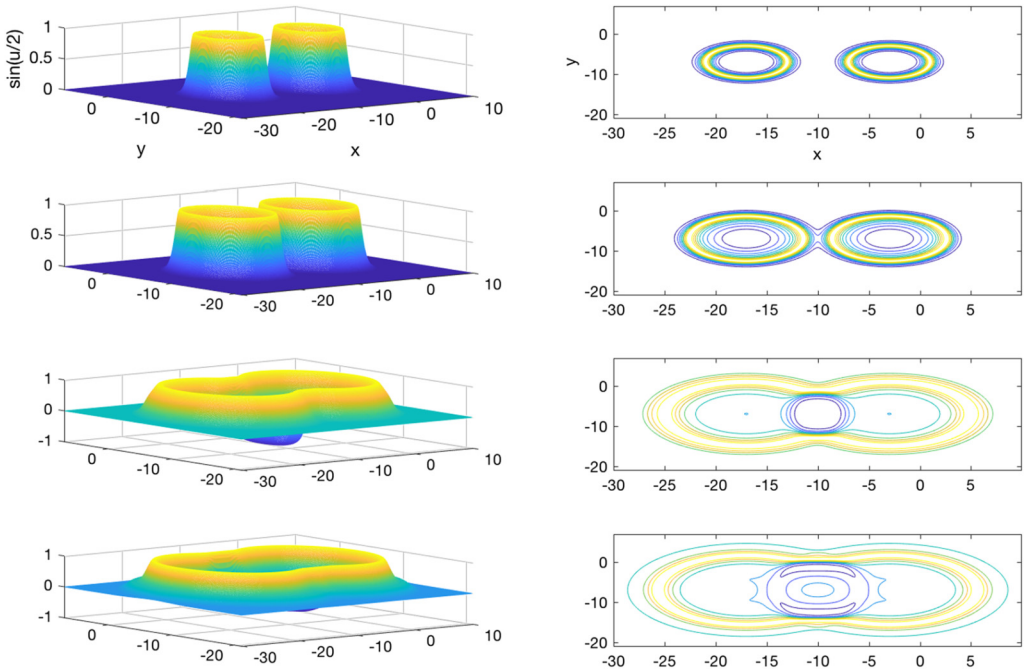

Fig. 8. Collision of two ring solitons at time $t = 0, 2, 6, 8$. Left: the surfaces of $\sin(u/2)$; Right: the contours of $\sin(u/2)$.

5. Conclusion

Many PDEs such as the KdV equation, Schrödinger-type equation, Sine Gordon equation, Maxwell's equations and so on belongs to the class of general multi-symplectic Hamiltonian systems, which possess some remarkable features such as they admit MSCL, LECL and LMCLs defined on any time-space region, independent of the boundary conditions. We developed

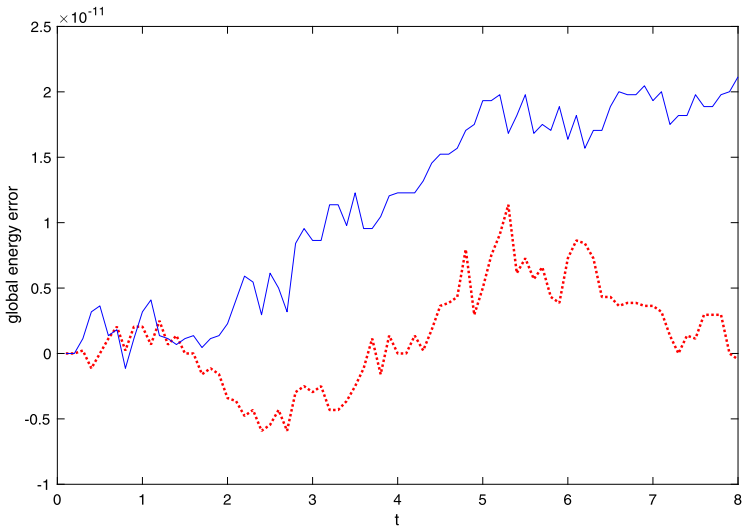

Fig. 9. The error in global energy. Solid line: LI-LEP-1; Dotted line: LI-LEP-2.

two classes of linearly implicit LEP schemes for the general multi-symplectic Hamiltonian systems. These schemes are second-order in both space and time, conserve local and global energies, and only require solving linear equations at each time step. Thus, our schemes are much more efficient than existing fully implicit schemes.

To demonstrate the effectiveness of our integrators, we applied them to solve the KdV equation, Schrödinger-type equations and Sine-Gordon in one and two dimensions. Our numerical experiments and comparisons with some existing schemes confirmed the efficiency and accuracy of our schemes and their advantages over existing schemes.

This study is mainly focused on the construction of linearly implicit LEP integrators for the general multi-symplectic Hamiltonian systems, further numerical analysis for these schemes will be carried out in a future work.

Declaration of competing interest

The authors declare that they have no known competing financial interests or personal relationships that could have appeared to influence the work reported in this paper.

Acknowledgements

The work of J. Cai is supported by Natural Science Foundation of Jiangsu Province of China (BK20181482), Qinglan Project of Jiangsu Province of China and Jiangsu Overseas Visiting Scholar Program for University Prominent Young & Middle-aged Teachers and Presidents. The work of J. Shen is supported in part by NSF grants DMS-1620262, DMS-1720442 and AFOSR grant FA9550-16-1-0102.

References

[1] U.M. Ascher, R.I. McLachlan, On symplectic and multisymplectic schemes for the KdV equation, J. Sci. Comput. 25 (2005) 83–104.
[2] U.M. Ascher, R.I. McLachlan, Multisymplectic box schemes and the Korteweg-de Veries equation, Appl. Numer. Math. 48 (2004) 255–269.
[3] W. Bao, Y. Cai, Optimal error estimates of finite difference methods for the Gross-Pitaevskii equation with angular momentum rotation, Math. Comput. 82 (2013) 99–128.
[4] T.J. Bridges, S. Reich, Multi-symplectic integrators: numerical schemes for Hamiltonian PDEs that conserve symplecticity, Phys. Lett. A 284 (2001) 184–193.
[5] T.J. Bridges, S. Reich, Multi-symplectic spectral discretizations for the Zakharov-Kuznetsov and shallow water equations, Phys. D: Nonlinear Phenom. 152 (2001) 491–504.
[6] B. Byland, Multisymplectic Integration, Ph.D. Thesis, Massey University, New Zealand, 2007.
[7] J.X. Cai, A new explicit multisymplectic scheme for the regularized long-wave equation, J. Math. Phys. 50 (013535) (2009) 1–16.
[8] J. Cai, C. Bai, H. Zhang, Decoupled local/global energy-preserving schemes for the *N*-coupled nonlinear Schrödinger equations, J. Comput. Phys. 374 (2018) 281–299.
[9] J. Cai, J. Hong, Y.S. Wang, Local energy- and momentum-preserving schemes for Klein-Gordon-Schrödinger equations and convergence analysis, Numer. Methods Partial Differ. Equ. 33 (2017) 1329–1351.
[10] W. Cai, C. Jiang, Y. Wang, Structure-preserving algorithms for the two-dimensional sine-Gordon equation with Neumann boundary conditions, arXiv: 1809.0270v1, 2018.
[11] J. Cai, Y. Wang, H. Liang, Local energy-preserving and momentum-preserving algorithms for coupled nonlinear Schrödinger equations, J. Comput. Phys. 239 (2013) 30–50.
[12] J. Cai, Y. Wang, C. Jiang, Local structure-preserving algorithms for general multi-symplectic Hamiltonian PDEs, Comput. Phys. Commun. 235 (2019) 210–220.

[13] J.R. Cavalcanti, M. Dumbser, D. Marques, C.R.F. Junior, A conservative finite volume scheme with time-accurate local time stepping for scalar transport on unstructured grids, Adv. Water Resour. 86 (2015) 217–230.
[14] J.B. Chen, M.Z. Qin, Multi-symplectic Fourier pseudo spectral method for the nonlinear Schrödinger equation, Electron. Trans. Numer. Anal. 12 (2001) 193–204.
[15] P.L. Christiansen, P.S. Lomdahl, Numerical solution of $2+1$ dimensional Sine-Gordon solitons, Phys. D 2 (1981) 482–494.
[16] D. Cohen, B. Owren, X. Raynaud, Multi-symplectic integration of the Camassa-Holm equation, J. Comput. Phys. 227 (2008) 5492–5512.
[17] M. Dahlby, B. Owren, A general framework for deriving integral preserving numerical methods for PDEs, SIAM J. Sci. Comput. 33 (2011) 2318–2340.
[18] Y. Gong, J. Cai, Y. Wang, Some new structure-preserving algorithms for general multi-symplectic formulations of Hamiltonian PDEs, J. Comput. Phys. 279 (2014) 80–102.
[19] O. Gonzalez, J.C. Simo, On the stability of symplectic and energy-momentum algorithms for nonlinear Hamiltonian systems with symmetry, Comput. Methods Appl. Mech. Eng. 134 (1996) 197–222.
[20] J. Hong, S. Jiang, C. Li, Explicit multi-symplectic methods for Klein-Gordon-Schrödinger equations, J. Comput. Phys. 228 (2009) 3517–3532.
[21] A.L. Islas, C.M. Schber, Multi-symplectic methods for generalized Schrödinger equations, Future Gener. Comput. Syst. 19 (2003) 403–413.
[22] T. Itoh, K. Abe, Hamiltonian-conserving discrete canonical equations based on variational difference quotients, J. Comput. Phys. 76 (1998) 85–102.
[23] C. Jiang, W. Cai, Y. Wang, A linear-implicit and local energy-preserving scheme for the sine-Gordon equation based on the invariant energy quadratization approach, J. Sci. Comput. 80 (2019) 1629–1655.
[24] L. Kong, J. Hong, J. Zhang, Splitting multisymplectic integrators for Maxwell's equations, J. Comput. Phys. 229 (2010) 4259–4278.
[25] L. Kong, P. Wei, Y. Hong, P. Zhang, P. Wang, Efficient energy-preserving scheme of the three-coupled nonlinear Schrödinger equation, Math. Method Appl. Sci., https://doi.org/10.1002/mma.5580, 2019.
[26] B. Leimkuhler, S. Reich, Simulating Hamiltonian Dynamics, Cambridge University Press, UK, 2004.
[27] T. Matsuo, D. Furihata, Dissipative or conservative finite-difference schemes for complex-valued nonlinear partial differential equations, J. Comput. Phys. 171 (2001) 425–447.
[28] R.I. McLachlan, G.R.W. Quispel, N. Robidoux, Geometric integration using discrete gradients, Philos. Trans. R. Soc. A 357 (1999) 1021–1046.
[29] R.I. McLachlan, M.C. Wilkins, The multi-symplectic diamond scheme, SIAM J. Sci. Comput. 37 (2015) A369–A390.
[30] B.E. Moore, S. Reich, Backward error analysis for multi-symplectic integration methods, Numer. Math. 95 (2003) 625–652.
[31] Z. Mu, Y. Gong, W. Cai, Y. Wang, Efficient local energy dissipation preserving algorithms for the Cahn-Hilliard equation, J. Comput. Phys. 374 (2018) 654–667.
[32] G.R.W. Quispel, D.I. McLaren, A new class of energy-preserving numerical integration method, J. Phys. A 41 (045206) (2008) 1–7.
[33] F.A. Radu, K. Kumar, J.M. Nordbotten, L.S. Pop, A robust, mass conservative scheme for two-phase flow in porous media including Höoder continuous nonlinearities, IMA J. Numer. Anal. 38 (2018) 884–920.
[34] J. Shen, J. Xu, J. Yang, The sclar auxiliary variable (SAV) approach for gradient flows, J. Comput. Phys. 353 (2018) 407–416.
[35] J. Shen, J. Xu, J. Yang, A new class of efficient and robust energy stable schemes for gradient flows, SIAM Rev. 61 (2019) 474–506.
[36] Q. Sheng, A.Q.M. Khaliq, D.A. Voss, Numerical simulation of two-dimensional Sine-Gordon solitons via a splitting cosine scheme, Math. Comput. Simul. 68 (2005) 355–373.
[37] W. Shi, X. Wu, J. Xia, Explicit multi-symplectic extended leap-frog methods for Hamiltonian wave equations, J. Comput. Phys. 231 (2012) 7671–7694.
[38] Y. Sun, P.S.P. Tse, Symplectic and multisymplectic numerical methods for Maxwell's equations, J. Comput. Phys. 230 (2011) 2076–2094.
[39] Y.S. Wang, B. Wang, M.Z. Qin, Local structure-preserving algorithms for partial differential equations, Sci. China Ser. A, Math. 51 (2008) 2115–2136.
[40] Linear Yang, Linear, first, and second-order unconditionally stable numerical schemes for the phase field model of homopolymer blends, J. Comput. Phys. 327 (2016) 294–316.
[41] X. Yang, L. Ju, Efficient linear schemes with unconditional energy stability for the phase field elastic bending energy model, Comput. Methods Appl. Mech. Eng. 315 (2017) 691–712.
[42] P.F. Zhao, M.Z. Qin, Multisymplectic geometry and multisymplectic Preissmann scheme for the KdV equation, J. Phys. A, Math. Gen. 33 (2000) 3613–3626.
[43] H. Zhu, L. Tang, S. Song, Y. Tang, D. Wang, Symplectic wavelet collocation method for Hamiltonian wave equations, J. Comput. Phys. 229 (2010) 2550–2572.